OPPOSITE SIDE ERS-1 SAR STEREO MAPPING OVER ROLLING TOPOGRAPHY

Thierry Toutin

Canada Centre for Remote Sensing

588 Booth Street

Ottawa, Ontario, Canada K1A 0Y7

ABSTRACT

Opposite-side radar stereo images have been considered unsuitable for stereo viewing due to illumination differences which limit the ability to identify the same features in the image pair. In some context, like a rolling topography (slope less than 10°), the shadow, layover foreshortening effects, specific to radar images, will not be overwhelming with an opposite-side stereo pair. This paper reports on some issues of stereo viewing and plotting, as well as on quantitative results of mapping and features extraction from ascending and descending orbit ERS-1 SAR stereo images. Planimetric accuracy of 17 m and altimetric accuracy of 23.9 m have been achieved for lake shorelines and DEM extractions, respectively. Impacts of different parameters on the accuracy are also evaluated.

INTRODUCTION

The prevailing multidisciplinary interest in planimetric and altimetric (elevation) data on surface terrain has governed research in the field of radar mapping. The possibility of using stereo-plotters (analog, analytical or digital) to obtain measurable models in three dimensions has long intrigued image interpreters for studies in such fields as topographic mapping, resource exploration and development, geological and

hydrological research, and has now increased with the development of geographic information systems (GIS). Stereo viewing enhances interpretability due to three-dimensional viewing, and enables planimetric feature extraction in the cartographic coordinate system without a digital elevation model (DEM). It can also be used for the generation of a DEM.

Improvement of synthetic aperture radar (SAR) systems, with parallel investigations into the theory, have allowed the demonstration of stereo radar with same-side or opposite-side viewing. As reported by Fullerton *et al.* (1986), theoretical studies (La Prade, 1963; Rosenfield, 1968; Gracie *et al.*, 1970; Leberl, 1972) and practical experiments (DBA-System, 1974; Derenyi, 1975; Graham, 1975; Leberl, 1976) confirm that the opposite-side stereo configuration is superior to same-side stereo configuration. Figure 1 illustrates the intersection geometry with the radar parallax due to elevation for both configurations. The difficulty in using this geometrically superior configuration comes from the illumination differences that are too pronounced to be stereoscopically viewed and the ability to find corresponding points and features.

Most of past experiments put the emphasis on developing same-side stereo methods, as reported by Leberl (1990). Recent developments of new systems such as ERS-1, ERS-2, JERS-1, Almaz, and in the future Radarsat will give us more opportunity to get an opposite-side stereo pair from ascending and descending orbits. Our goal is to show the usefulness and the applicability of this approach. This paper briefly outlines some issues on stereo viewing and plotting, examines the problems and compromises for obtaining good geometry and radiometry together, and ways of overcoming these problems. Then, using a rigorous photogrammetric solution already developed at the Canada Centre for Remote Sensing (CCRS) (Toutin and Carboneau, 1992; Toutin, 1994) on a digital stereo workstation, the DVP, results and accuracies of planimetric

and altimetric features extraction with ERS-1-SAR stereo images from ascending and descending orbits are presented and analyzed.

STEREO VIEWING AND PLOTTING ISSUES

Since the early studies on SAR stereo viewing, these issues have been well analyzed and documented by various authors (La Prade, 1970; Graham, 1975; Fullerton *et al.*, 1986; Kobrick *et al.*, 1986; Leberl, 1990; Yelizavetin, 1993). They can be separated into geometric and radiometric issues.

To obtain good geometry for a better stereo plotting, the intersection angle[1] (Figure 1) should be large in order to increase the stereo exaggeration factor or, equivalently the observed parallax, which is used to determine the terrain elevation. Conversely, to have good stereo viewing, the interpreter prefers a stereo pair as nearly identical as possible, implying a small intersection angle. Furthermore, large variations of the intersection angle generate non-linear variations in the scales of the stereo pair along the range direction, resulting in an additional "parasitic" displacement of the corresponding points. This last issue is mainly valid for airborne SAR stereo images (Yelizavetin, 1993; Toutin, 1995). For crossing flight lines, the angle of convergence[1] between the two lines should be less than about 40 degrees (Kobrick *et al.*, 1986) to keep the stereo impression. However, without a careful evaluation of the types of images (incidence and intersection angles), of the stereo configuration (same-side and opposite-side viewings), and of the ground relief, it is not meaningful to generalize to other stereo experiments.

[1] The intersection angle is the difference between the two incidence angles, and the convergence angle is the difference between the two orbit track angles.

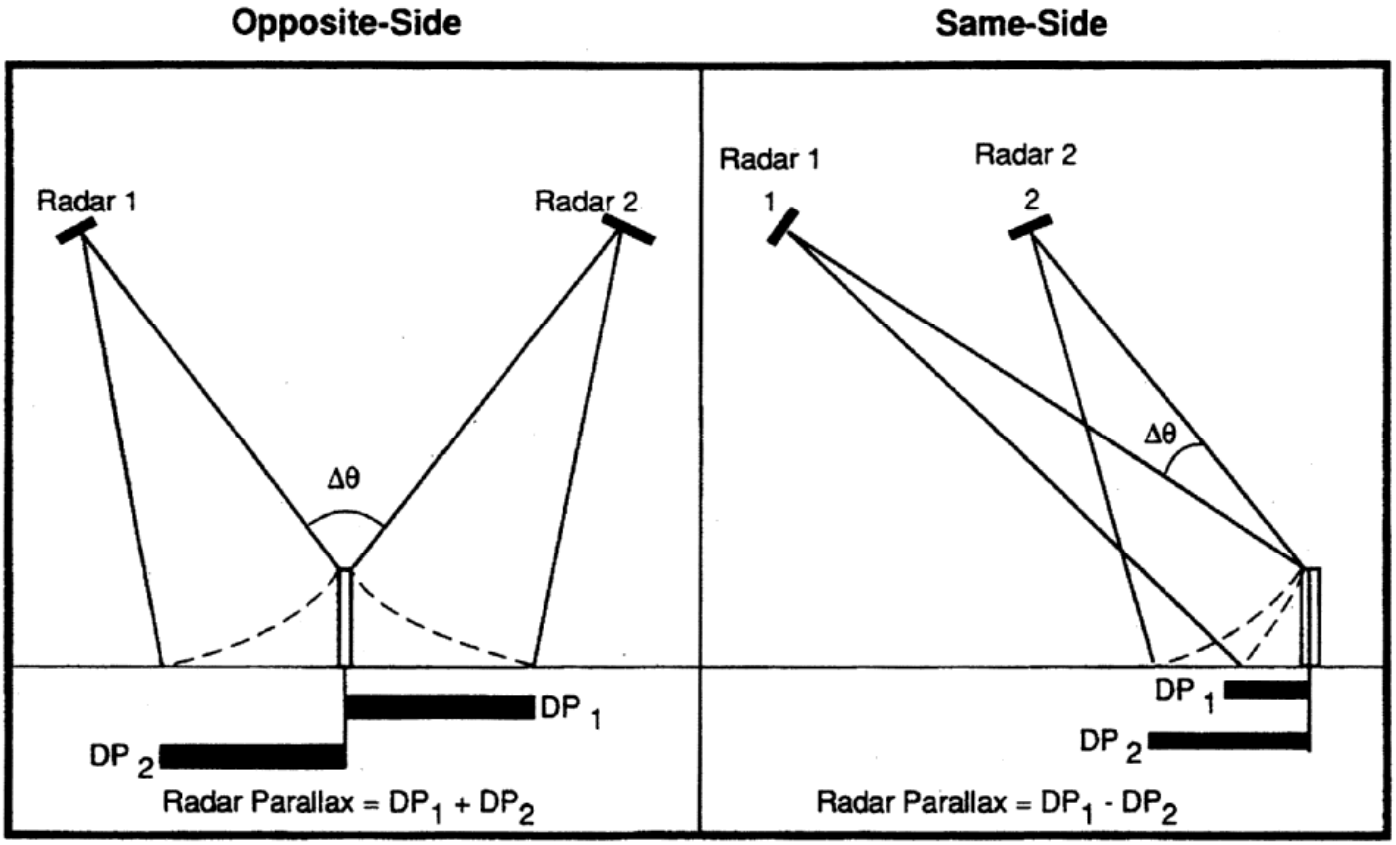

Figure 1:Radar parallax with the opposite- and same-side configuration ($\Delta\theta$ = intersection angle).

In terms of radiometry, what parameters can affect the stereo viewing and the stereo pointing? Fullerton et. al. (1986) demonstrates that the observer can adjust to global brightness difference, but additional contrast is sometimes necessary to obtain good consistency between the two images (Yelizavetin, 1993). All frequencies are needed for stereoscopy because the lack of lower frequency makes stereo viewing very difficult, and the lack of higher frequency does not make precise pointing possible (Fullerton *et al.*, 1986). The presence of speckle on SAR images decreases the quality in the stereo viewing and plotting, because it blurs outlines, increasing the difficulty of perception and plotting of the small terrain details.

Consequently, both large geometric and radiometric disparities on the stereo pair hinder stereo viewing and precise stereo plotting. As a reduction of one disparity could compensate for the other disparity, a compromise has to be reached between a better stereo viewing (small radiometric differences) and a stronger stereo geometry and plotting (large parallax).

The common compromise is to use a same-side stereo pair, which reduces both disparities. But, to reduce the radiometric difference of an opposite-side stereo pair, Yoritomo (1972) and Fullerton (1986) inverted the radiometry of one image. Fullerton *et al.* (1986), processing digital images, added a local brightness change to exclude some image features from the radiometric inversion. In another way to reduce the geometric difference, the images can be geometrically pre-processed with a low frequency or a sparse digital elevation model (DEM). This technique to reduce the parallax difference has been already applied with success to iterative hierarchical image matching (Simard *et al.*, 1986).

In our study, the compromise is to have a stronger stereo geometry with opposite-side ERS-1 SAR stereo pair from ascending and descending orbits over a rolling topography study site. The rolling topography reduces the parallax difference, and since there is no layover, no shadow and a few foreshortening it also reduces the radiometric disparities between the two images, making possible the stereo viewing and a good stereo plotting.

STUDY SITE AND DATA SET

The study site located north of the Sudbury Basin (Ontario, Canada) overlaps four 1:50 000 topographic maps. This terrain is characterized by rolling topography where the

elevation ranges from 300 m to 500 m, and slopes generally do not exceed 10 degrees. The land cover consists mainly of a forest mix of coniferous and deciduous trees approximately 10 metres tall. Lakes and ponds are numerous and they are connected through a series of small rivers with gentle shorelines. The relief is typical of the Canadian shield of Quebec and Ontario.

The remote sensing data consists of two ERS-1 SAR images acquired on August 22 and 28, 1992 from ascending and descending orbits, respectively. The stereo coverage is about 50 km by 50 km. Both images are in ground range presentation with a 12.5-m pixel spacing. Images have been linearly compressed from 16 bits to 8 bits; an antenna pattern correction has been applied, and a 5 x 5 Lee filter has been used to reduce the speckle. It increases, as mentioned earlier, the quality of the stereo viewing and plotting.

These images are SAR standard products generally available to users. They are generated digitally during post processing from the raw signal SAR data (Doppler frequency, time delay). Errors present in the input parameters to image geometry model will propagate through to the image data. These include errors in the estimation of slant range and of Doppler frequency and also errors due to the satellite's ephemeris data and the ellipsoid. Assuming the presence of some geometric error residuals, the parameters of the geometric correction model using a rigorous photogrammetric solution reflect these residuals (Toutin and Carbonneau, 1992).

The topographic data (hydrography and 10-m contour lines) was digitized by the University of New Brunswick (Canada) from a 1:20 000 topographic map. The planimetric and altimetric accuracies are 5 metres and the DEM has been generated with a 10-m accuracy.

A 30 km by 30 km area common to both the ERS-1 stereo model and the topographic data coverage was used for the evaluation of the stereo restitution. Since the ERS-1 SAR images and the topographic data were not taken at the same date and year, some discrepancies are noted in the lake and pond shapes.

PROCESSING

The main steps of the processing are summarized in Figure 2.

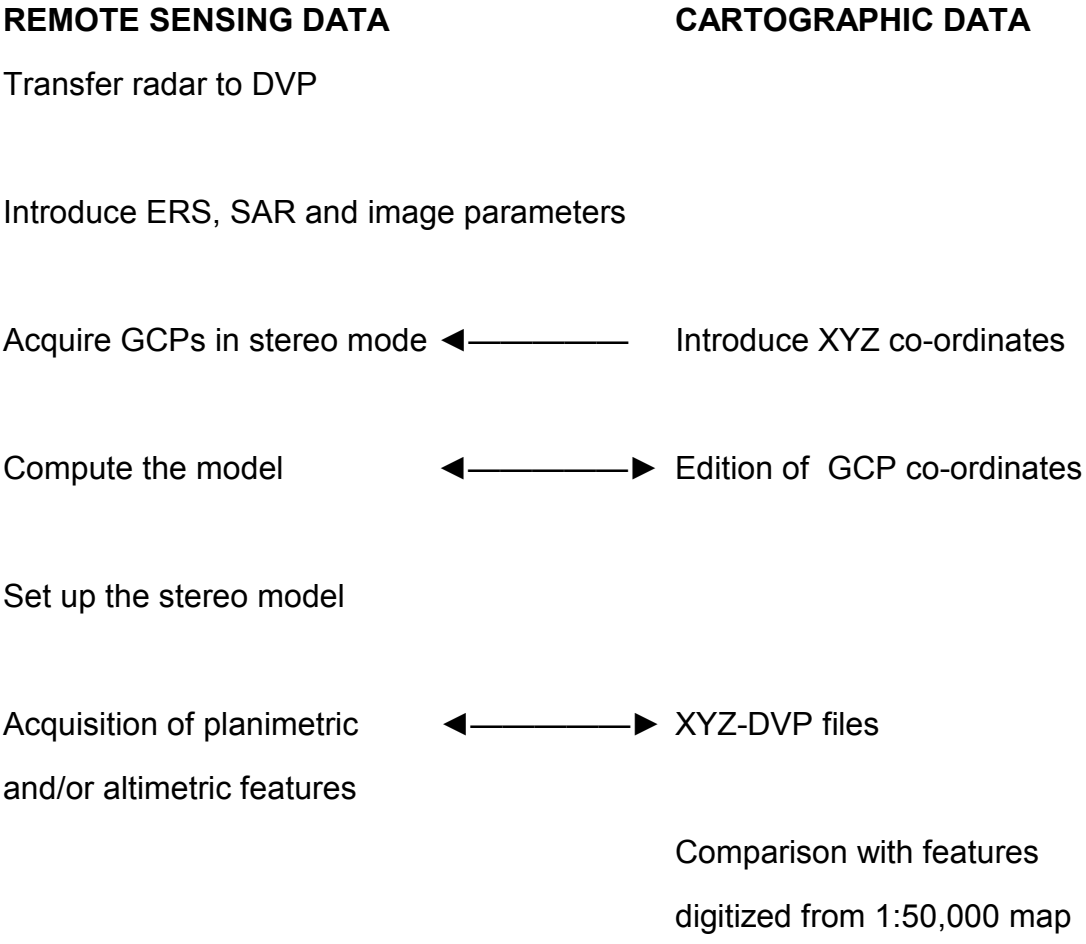

Figure 2: Processing steps

The digital stereo workstation (DVP), used in the processing, has been developed through co-operation between the Canada Centre for Remote Sensing (CCRS) and the Département des sciences géodésiques et de télédétection de l'Université Laval.

Evolved as a by-product of educational tools developed at Laval University, the DVP is now a low-cost general purpose digital stereo workstation. The objective for the first development was to create a system on common micro-computer hardware to solve standard photogrammetric problems in a user-friendly and efficient way (Gagnon *et al.*, 1990). Subsequently, the system has been adapted to process stereo remote sensing data: SPOT-HRV (Toutin *et al.*, 1993) and SAR data (Toutin, 1994).

Digital Transfer to the DVP

The image data was read from magnetic tapes, radiometrically pre-processed and transferred to the DVP. Parameters of the ERS platform (position, velocity), of the SAR sensor (resolution, angles), of the images (pixel spacing, image centre), and of the Earth (ellipsoid) are introduced interactively.

Stereo Model Set-up

Forty-four (44) ground points (rivers and lake shorelines) were first identified and plotted in stereoscopic mode on the ERS-SAR images. The image coordinate accuracy is 1-2 pixels (12-25 m). Then, the ground coordinates (XYZ) have been obtained directly from the digital topographic data with 5-m accuracy.

Twelve (12) points have been used as GCPs to compute the geometric modelling of the stereo pair with photogrammetric techniques (collinearity and co-planarity conditions[2])

[2] The collinearity condition states that the exposure centre, the location of a ground point and its image point are colinear, and the coplanarity condition states that projection rays from both sensor positions for the same ground point are coplanar (Figure 1).

and by an iterative least square adjustment (Toutin and Carbonneau, 1992). The resulting root mean square (RMS) residuals on the twelve GCPs are 18.3 m, 15.6 m and 6.5 m in X, Y and Z direction, respectively. The 32 remaining points have been used as independent check points. The RMS errors are 24.9 m, 17.9 m and 9.2 m in X, Y and Z direction, respectively. Previous studies with SEASAT-SAR (Toutin and Carbonneau, 1992) have shown that this geometric modelling is not affected by the number and the spatial distribution of the GCPs, because it respects the global viewing geometry (sensor + platform + Earth). The residuals reflect the modelling accuracy, and the errors the restitution accuracy. As the RMS residuals and errors are in the same order of magnitude as the plotting error (1-2 pixels), the mathematical model properly describes the viewing geometry of the SAR stereo pair.

As a result, the stereo model is generated directly from the raw images without any resampling. The Y-parallax between the two images is automatically cancelled at the floating marks when the operator moves in the stereo model. When the operator cancels the X-parallax to fuse the two floating marks at the measured point, a 3-D stereo intersection is performed using the previously computed geometric modelling to convert the pixel coordinates in both images of the stereo pair to three-dimensional data. Cartographic coordinates (planimetry and height) in the user defined map projection system are determined in real time for the measured point with a least-squares intersection process based on the geometric modelling equations and parameters (Toutin *et al.*, 1993).

Data Extraction in the Stereo Model

Once the stereo model has been set up, the stereo data extraction follows. It is done visually and interactively by the operator. On this ERS-1 SAR stereo model, few features were identifiable due to low contrast in the SAR data, the roads, railroads and

rivers were only intermittently visible for extraction and this hindered accuracy evaluation. The forest covered the full stereo model and thus only lake shorelines have been digitized in stereoscopy from the 12.5-m pixel spacing.

For the altimetry, the height measurements are extracted on a ten-pixel regular grid on the left image: this generates an irregular grid of points when projected to the ground system.

Transfer to the GIS System

DVP XYZ files are transferred to ARC/INFO using a bi-directional translator developed by ESRI Canada in Montreal. The vector data are cleaned and edited using different GIS functions of ARC/INFO, and then compared to the topographic data. The irregular DEM, transferred as a point file, is used to generate a triangular irregular network (TIN). Lakes are also used to refine the interpolation of the TIN. This TIN is then transformed into a 50-m grid file. Similarly, for the topographic data, an IGDS/ARC translator is used to import the topographic files into the ARC/INFO environment. Only data common to both the topographic data and the SAR stereo model on the DVP were retained.

RESULTS AND DISCUSSION

Two hundred lakes with a total of 322 km perimeter have been extracted. A first comparison has been done between the map file and the DVP file to compute the omission and commission errors. The commission error comes from the over-estimation of lakes, and the omission error from the under-estimation. There is no commission error and the 30% omission error results from intermittent marshes and swamps. The lakes, rivers and other water bodies are very separable from the wetlands and forest, unless wind induced surface roughness increases the backscatter.

Wetlands (marshes, swamps,...) with significant open water also exhibit this phenomenon which causes confusion with forest. Furthermore, vegetated wetlands generally appear similar to forest.

In a second step, buffered zones centred on the map features were generated at 5, 10, 15, 20, 25, 30, 35, 40, 45 and 50 m. These buffered zones are corridors "parallel" to lake shorelines at different distances; they are used to quantify the cumulative linear distance of stereo-extracted DVP features within each zone. The percentage and the cumulative percentage of linear distance can then be computed for each zone. Table 1 gives the general results: it shows a 17-m RMS accuracy and a 31-m accuracy with 90% confidence. Table 1 also shows that there is no bias (larger than 5 m) because the percentage for each 5-m zone decreases from the "0-5" zone to the "over-50" zone. At the bottom of Table 1, one can note that 4.4% have errors greater than 40 metres. By displaying only these errors on the DVP, it may be seen that the origins of these errors are the interpretation of the limit between lakes and swamps, and mainly the variation in shape: lakes "shrank" during the summer period. On the ERS-1 SAR image, the shape of the lake is determined by the current shoreline, because the "high water limit" is not visible.

The impact of different parameters on the accuracy have been evaluated by generating other statistics. The first parameters are the orientation of the shoreline according to the satellite paths (perpendicular vs parallel; east vs west), and the location in the stereo model. By computing the different statistics within each buffered zone, it was noted that there is no significant difference to conclude that one orientation or location in the stereo model gives a better accuracy.

Accuracy (metres)	Distance (metres)	Percentage (%)	Cumulative Percentage
5	73 347.5	22.8	22.8
10	66 389.7	20.6	43.4
15	54 308.1	16.9	60.3
20	42 425.4	13.2	73.5
25	30 381.5	9.4	82.9
30	19 402.7	6.0	88.9
35	13 023.6	4.0	92.9
40	8 780.3	2.7	95.6
45	5 514.0	1.7	97.3
50	3 161.4	1.0	98.3
50+	5 430.3	1.7	100.0
TOTAL	322 164.0		100.0

Table 1: Stereo Restitution Accuracy of all the lakes

The third parameter is the size of the lakes, because, visually, larger lakes seem to be better defined. Three large lakes (perimeter of about 18 km each and surface of about 2 km^2) and 17 small lakes (perimeter of about 0.6 km each and surface of about 0.02 km^2), present in the stereo model were used to generate the statistics (Table 2).

Table 2 shows 15-m and 16-m RMS accuracies, and 29-m and 29-m accuracies with 90% confidence for the large and small lakes, respectively. As shown with the previous statistics (Table 1), there is no bias larger than 5 m. These results are on the same order of magnitude as the results for all the lakes together (Table 1), indicating the size of the lakes doesn't affect the stereo extraction accuracy.

Accuracy (metres)	Large Lakes			Small Lakes		
	Distance (metres)	Percentage (%)	Cumulative Percentage	Distance (metres)	Percentage (%)	Cumulative Percentage
5	12 408.0	25.4	25.4	2 383.6	24.3	24.3
10	11 554.8	23.7	49.1	2 231.7	22.7	47.0
15	8 326.0	17.2	66.3	1 667.6	17.0	64.0
20	5 801.7	11.9	78.2	1 047.6	10.7	74.7
25	3 994.6	8.2	86.4	937.8	9.5	84.2
30	2 216.0	4.5	90.9	684.9	7.0	91.2
35	1 488.4	3.0	93.9	408.8	4.2	95.4
40	958.7	2.0	95.9	224.0	2.3	97.7
45	744.2	1.5	97.4	66.1	0.7	98.4
50	443.3	0.9	98.3	61.9	0.6	99.0
50+	816.8	1.7	100.0	106.6	1.0	100.0
TOTAL	48 802.5		100.0	9 820.5		100.0

Table 2: Stereo Restitution Accuracy for 3 Large Lakes and 17 Small Lakes

The use of opposite-side stereo images is one of the major factors for explaining these results: good accuracies, consistency and robustness over the stereo model, and non-sensitivity to different geometric parameters. The images from ascending and descending orbits are complementary in terms of geometry and radiometry.

The stronger geometry enables larger parallaxes to be produced, and consequently a better accuracy (17 m) to be achieved. These results are consistent with the accuracy evaluation from previous experiments: subresolution accuracy for opposite-side vs accuracy of a few resolution cells for same-side stereo pair (Fullerton *et al.*, 1986).

The opposite viewing (east looking and west looking) enables the different orientations of the shoreline to be extracted with the same accuracy. In the stereo viewing and

plotting the "best information" of each image is used by the operator. As there is generally less wind during the night, it gives different radiometric contrasts for lakes, wetland and forests features between the two images. This complementarity enables a better determination of those different features. Furthermore, as the small variation (few degrees) of the intersection angle in the stereo model doesn't generate non-linear variations in the scales of the stereo pair along the range direction, it gives a good consistency and robustness in the full stereo model.

For the height measurements, a first evaluation was performed to quantify the relative pointing error. Twenty points, which span different features and cover type, were chosen. It should be noted that these are not necessarily identifiable features. Pointing of these points ten times leads to a ± 2.7-m pointing error. Furthermore, 100 check points with known ground coordinates (accuracy of five metres) are plotted on the stereo model to quantify the absolute altimetric accuracies at spot points. Fifty were well-identifiable points like lake shorelines and rivers, and fifty were spread over the forest (the tree height is only 10 m). For the first group, the accuracy in X, Y, and Z direction are 11.2 m, 14.5 m and 14.1 m, respectively. For the second group, the accuracy in Z is 23.1 m. It is worth noting that the stereo images have a base-to-height ratio of 0.85, and the altimetric digitizing accuracy with a 12.5-m pixel spacing is ± 8 metres. A bias of ten metres has also been observed.

The difference in the altimetric accuracies between the two groups comes from:

- the forest lacks defined spot points, so the error in plotting is larger (±1-2 pixels), and

- since C-band microwave does not penetrate the forest canopy, variation in canopy height above the ground generates random error (±5 m).

The bias comes from the operator who plots always at a lowest altitude. It has been checked with other data (aerial photos and SPOT-panchromatic). This bias is specific for each operator in the stereo plotting, and can be computed for each type of data.

About 6 600 points (irregular DEM) are acquired on the stereo model and directly compared to the DEM generated from the 10-m contour lines with ARC/INFO functions. This avoids errors generated by any processing to transform this irregular DEM into a regular grid. The statistics generated from these points give:

RMS error = 23.9 m	Error min. = - 72.0 m
Bias = + 11.5 m	Error max. = + 123.1 m

Compared to the absolute altimetric errors computed previously (14.1 m for well-identifiable points and 23.1 m for "forest" points), the 23.9 m RMS error for the DEM is consistent, but some of these errors (1.5%) are large. By displaying on the DVP the points (only 100 over 6 600) which are out of tolerance, it may be seen that they are spatially grouped and not randomly distributed in the stereo model. Since the radiometric disparities between the two opposite side stereo images have been reduced with the rolling topography (no layover, no shadow, few foreshortening), these 1.5% errors are mainly human errors due to different reasons (operator's fatigue, poor contrast, speckle, etc.). Replotting these points stereoscopically confirms this statement, because the results improve. Figure 3 is a part of the stereo pair, and shows an area (between the white corners, at the top left), where such large errors occur; one can note few disparities between the two opposite-side images which have made easier the stereo-viewing and plotting.

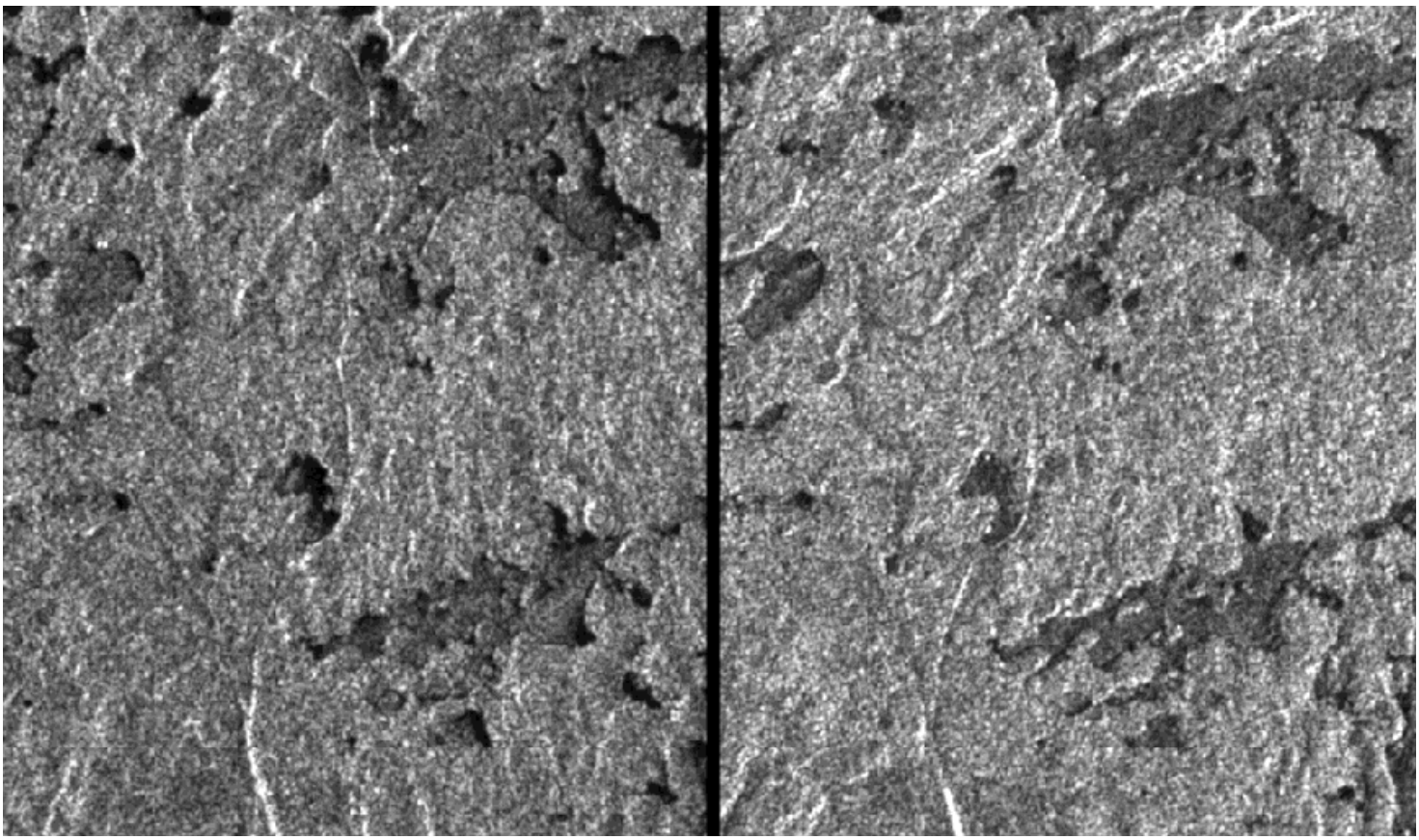

Figure 3: Example of ERS-1 SAR opposite-side stereo pair (between the white corners at the top left, some 100-m altimetric error points occurred).

CONCLUSIONS

With SAR images, opposite-side stereo can provide the best geometry, but most of the time the radiometric and visual problems negate these advantages. The trade-off is then to decide between easier fusion of a stereo model or greater vertical exaggeration. The trade-off chosen in this study was an opposite-side SAR stereo pair from ascending and descending orbits over a rolling topography, which provided a stronger geometry and a good fusion of the stereo model, because the radiometric disparities due to layover, shadow, and foreshortening effects have been reduced.

This paper has then presented quantitative results of data extraction in planimetry and altimetry from opposite-side ERS-1 SAR stereo images on a PC-based stereo workstation using a photogrammetric approach. The mathematical equations, which drive the DVP, are based on the collinearity and co-planarity conditions. They represent the physical reality of the full viewing geometry: platform-sensor-Earth.

From the raw images, the data are interactively stereo-extracted and transferred to a GIS environment. Compared to digital topographic data, planimetric and altimetric accuracies have been computed for lake shorelines and for an irregular DEM.

In planimetry, the lake shoreline accuracy is 17 metres. The orientation of the shoreline, the location and the size of the lake do not have an effect on this accuracy. In altimetry, an accuracy of 23.9 metres with a 10-m bias have been computed for the DEM extraction. The bias is due to the operator who systematically stereo plotted at lower altitude. Although this phenomena is well known in stereo photogrammetry, it has to be confirmed with other data and study sites.

Some main issues for these good and consistent results (ie. equal to or better than the SAR resolution) have been demonstrated:

- a strong geometry with opposite-side stereo pair;
- a good fusion with a rolling topography;
- a complementary aspect in radiometry with East-and-West looking images and day-and-night images.

A better knowledge of the backscatter phenomena (day vs night; lake vs swamp vs forest) should enable the operator to further reduce the omission error and to improve

the accuracy. This complementarity of different geometries and time acquisition has to be studied further to more effectively use this technique.

As this study site with its rolling topography is typical of the Canadian shield, the proposed method is not a specific case, but can be applied over larger areas in Canada and also around the world if the site has about the same characteristics (rolling topography, slope, convergence angles, etc.).

Furthermore, when geometric distortions caused by relief are too important for the fusion, it is possible to optimize it by a hierarchical process called "stereo reduction" (Fullerton *et al.*, 1986; Simard *et al.*, 1986). The radar images have to be geometrically rectified with a coarse DEM to reduce the excessive parallaxes. It is not important that this coarse DEM be accurate, because it will be refined with more accurate measurements in the "reduced stereo model". Future studies will evaluate the accuracy and the limit of such an hierarchical process with opposite-side stereo images.

ACKNOWLEDGEMENTS

The author would like to thank his CCRS colleagues, Brian Brisco and Laurence Gray for their critical review to improve this paper. He also thanks M. Benoît Rivard who produced the pre-processed data and for his comments, and Ms Liyuan Wu of Consultants TGIS inc., for the data acquisition.

REFERENCES

DBA-Systems. 1974. Research, Studies and Investigations for Radar Control Extensions. DBA Systems Inc., **Defence Documentation Center Report No. 530784L**, Florida, U.S.A.

Derenyi, E.E. 1975. Topographic Accuracy of Side Looking Radar Imagery. **Bildmessung und Luftbildwesen**, Vol. 32, No. 1, pp. 68-78.

Fullerton, J.K., F. Leberl and R.E. Marque. 1986. Opposite-side SAR Image Processing for Stereo Viewing. **Photogrammetric Engineering and Remote Sensing**, Vol. 52, No. 9, September 1986, pp. 1487-1498.

Gagnon, P.A., J.P. Agnard, C. Nolette and M. Boulianne. 1990. A Microcomputer-based General Photogrammetric System. **Photogrammetric Engineering and Remote Sensing**, Vol. 56, No. 5, pp. 623-625.

Gracie, G., J.W. Bricker, R.K. Brewer and R.A. Johnson. 1970. Stereo Radar Analysis, **U.S. Engineer Topography Laboratory Report No. FTR-1339-1**, Ft. Belvoir, U.S.A., 70 pages.

Graham, L. 1975. Flight Planning for Radar Stereo Mapping. **Proceedings American Society of Photogrammetry**, 41st Annual Convention, Washington, D.C.

Kobrick, M., F. Leberl and J. Raggam. 1986. Radar Stereo Mapping with Crossing Flight Lines. **Canadian Journal of Remote Sensing**, Vol. 12, No. 9, pp. 132-148.

La Prade, G.L. 1963. An Analytical and Experimental Study of Stereo for Radar. **Photogrammetric Engineering**, Vol. 29, pp. 294-300.

La Prade, G.L. 1970. Subjective Considerations for Stereo Radar. **Goodyear Aerospace Corp.**, Report G1B-9169.

Leberl, F. 1972. On Model Formation with Remote Sensing Imagery. **Oesterreichisches Zeitung für Vermessungswesen**, Vol. 601, No. 2, pp. 43-61.

Leberl, F. 1976. Imaging Radar Applications to Mapping and Charting. **Photogrammetria**, Vol. 32, No. 3, pp. 75-100.

Leberl, F. 1990. Radargrammetric Image Processing, **Artech House**.

Rosenfield, G.H. 1968. Stereo Radar Techniques. **Photogrammetric Engineering**, Vol. 34, pp. 586-594.

Simard, R., F. Plourde, and Th. Toutin. 1986. Digital Elevation Modelling with Stereo SIR-B Image Data, **Proceedings of the 7th International Symposium on Remote Sensing for Resources Development and Environmental Management**, ISPRS Commission VII, Enochede, 25-29 August, pp. 161-166.

Toutin, Th., and Y. Carbonneau. 1992. MOS and SEASAT Image Geometric Corrections. **IEEE Transactions on Geoscience and Remote Sensing**, Vol. 30, No. 3, pp. 603-609.

Toutin, Th., Cl. Nolette, Y. Carbonneau et P.A. Gagnon. 1993. Stéréo-restitution interactive des données SPOT : description d'un nouveau système. **Journal canadien de télédétection**, Vol. 19, No. 2, pp. 146-151.

Toutin, Th. 1994. Cartographie à partir d'images radar. **Journal canadien de télédétection**. Vol. 20, No. 2, pp. 171-179.

Toutin, Th. 1995. Airborne SAR Stereo Restitution in a Mountainous Area of Costa Rica: First Results. **IEEE Transactions on Geoscience and Remote Sensing**, Vol. 33, No. 2, pp. 500-504.

Yelizavetin, I.V. 1993. Digital Terrain Modelling from Radar Image Stereopairs. **Mapping Sciences and Remote Sensing**, Vol. 30, pp. 151-160.

Yoritomo, K. 1972. Methods and Instruments for the Restitution of Radar Pictures. **Invited Paper at the 12th Congress of the International Society for Photogrammetry**, Ottawa, Canada.